EUROPEAN ORGANIZATION FOR NUCLEAR RESEARCH

A METHOD FOR MEASURING TRANSVERSE COUPLING IMPEDANCE

G. Nassibian and F. Sacherer

## SUMMARY

It is relatively easy to measure the transverse impedance $Z_T$ for accelerator components with large impedance such as kicker magnets. Useful results can also be obtained for components with small impedance, such as vacuum chambers, although in this case one is close to the limits of accuracy with ordinary laboratory equipment. Finally, a relationship between longitudinal and transverse coupling impedance is derived that differs from the one usually assumed.

## CONTENTS

1.  INTRODUCTION

A beam that oscillates from side to side with amplitude $\pm\Delta$ induces differential currents and charges on the walls of the vacuum chamber. These in turn produce a transverse magnetic field B and electric field E which further deflect the beam. The thresholds for beam instability and the growth rates depend on the transverse coupling impedance[1]

$$Z_T = \frac{j}{\beta I \Delta} \int_0^{2\pi R} (E + v \times B)_T \, ds, \qquad (\Omega/m) \qquad (1)$$

where I is the beam current, v is the beam velocity, and $\beta = v/c$. In the following, we concentrate on magnetic deflection, although electric deflection is also important in some cases.

The source of the differential wall current is the dipole moment $I\Delta$ per unit length of the beam. The same wall currents and magnetic field B result if the beam is replaced by two parallel wires, or more simply by a loop of length $\ell$, width $\Delta$, and current I. The field B in turn induces the voltage

$$j\omega B \ell \Delta = ZI$$

in the loop, which increases its impedance by Z. If Z is measured, then

$$B = \frac{ZI}{j\omega\ell\Delta} \quad ,$$

and from (1),

$$Z_T = \frac{c}{\omega} \frac{Z}{\Delta^2} \qquad (2)$$

is the transverse impedance $(\Omega/m)$ for a length $\ell$ of structure. This is the basis for the measurements discussed in the following sections. Measurement techniques for determining the longitudinal impedance $Z_L$ are discussed elsewhere[2-5].

2.  RELATION BETWEEN $Z_T$ AND $Z_L$

Let $E_z(x, x_0)$ be the image field at x due to a current filament of intensity I at $x_0$. For a length $\ell$, define

$$Z_1(x, x_0) = \frac{\ell E_z(x, x_0)}{I} . \qquad (3)$$

This is a measurable quantity, which reduces in the limit $x \to x_0$ to the usual longitudinal impedance $Z_L$.

The image field from two filaments separated by $\Delta$ and carrying equal but opposite currents I is

$$E_z' = \frac{\partial E_z(x, x_0)}{\partial x_0} \Delta \quad ,$$

and the image magnetic field perpendicular to the plane of the filaments

$$B' = \frac{\Delta}{j\omega} \frac{\partial^2 E_z(x, x_0)}{\partial x \, \partial x_0}$$

is found by equating the integral of $E'_z$ around a contour of length $\ell$ and width $dx$,

$$\frac{\partial E'_z}{\partial x} \ell \, dx \ ,$$

to the rate of change of flux through the contour, $dx\ell\dot{B}'$. Insert $B'$ into (1) to find the transverse impedance,

$$Z_T = \frac{c}{\omega} \left. \frac{\partial^2 Z_1(x, x_0)}{\partial x \, \partial x_0} \right|_{x=x_0} , \tag{4}$$

while the longitudinal impedance is given by

$$Z_L = Z_1(x, x_0) \Big|_{x=x_0} . \tag{5}$$

For the examples which follow, $Z_L$ has the form

$$Z_L = \text{const} + F^2(x_0) \ , \tag{6}$$

so $Z_T$ can be obtained directly from the position dependence of $Z_L$,

$$Z_T = \frac{c}{\omega} \left( \frac{dF}{dx_0} \right)^2 . \tag{7}$$

This is not true in general, however. For example, a beam between two parallel infinite plates sees a constant $Z_L$ independent of position, with F everywhere zero, although $Z_T$ is non-zero. Further discussion of the relation between $Z_L$ and $Z_T$ can be found elsewhere[1,6-8].

## 3. CIRCULAR VACUUM CHAMBER

If the wall thickness is greater than the skin depth, a current filament of intensity I that is displaced by $x_0$ from the centre of a circular pipe induces the wall current density

$$J = \frac{I}{2\pi b} \frac{1 - \epsilon^2}{1 + \epsilon^2 - 2\epsilon \cos \theta} , \tag{8}$$

where $\epsilon = x_0/b$, and b is the pipe radius. For small $\epsilon$, this reduces to the usual $\cos \theta$ distribution,

$$J = \frac{I}{2\pi b} \left( 1 + 2 \frac{x_0}{b} \cos \theta \right) . \tag{9}$$

For finite wall resistivity, the electric field at the wall is $E_z = \mathcal{R} J$, where

$$\mathcal{R} = (1 + j)\frac{\rho}{\delta} \quad \text{(ohm per square)} \tag{10}$$

is the surface impedance, $\rho$ is the resistivity ($\Omega \cdot m$), and $\delta$ is the skin depth. The resulting longitudinal field in the pipe at x is

$$E_z = \frac{\mathcal{R} I}{2\pi b} \left(1 + 2 \frac{x_0 x}{b^2}\right) ,$$

giving

$$Z_1(x, x_0) = \frac{\ell \mathcal{R}}{2\pi b} \left(1 + 2 \frac{x_0 x}{b^2}\right) \tag{11}$$

for a length $\ell$. The impedances due to wall resistivity are therefore

$$Z_L = \frac{\ell \mathcal{R}}{2\pi b} \left(1 + 2 \frac{x_0^2}{b^2}\right) \tag{12}$$

and

$$Z_T = \frac{c}{\omega} \frac{\ell \mathcal{R}}{\pi b^3} \tag{13}$$

$$= \frac{2c}{\omega b^2} Z_L \bigg|_{x_0 = 0} \tag{14}$$

which are the known results.

The additional reactive impedance due to perfectly conducting walls can be found as follows. From (9), the wall current density due to two filaments separated by $\Delta$ and carrying equal and opposite currents I is

$$J = \frac{I}{2\pi b} \frac{2\Delta}{b} \cos \theta , \tag{15}$$

which in turn produces a uniform vertical magnetic field

$$B = \frac{\mu_0 I}{2\pi b} \frac{\Delta}{b} ,$$

leading to

$$Z_T = -j \frac{Z_0}{2\pi b^2} , \tag{16}$$

where $Z_0 = 120\pi \ \Omega$ is the impedance of free space. The complete expression[9,10]

$$Z_T = -j \frac{Z_0}{2\pi} \left( \underset{\uparrow}{\frac{1}{\beta^2}} - \underset{\uparrow}{1} \right) \times \left( \underset{\uparrow}{\frac{1}{a^2}} - \underset{\uparrow}{\frac{1}{b^2}} \right) \tag{17}$$

$$\text{electric} \quad \text{magnetic} \quad \text{beam} \quad \text{wall}$$

includes the effect of the electric field $E = \beta^{-1} B$ and the direct action of the beam of radius a on itself. The latter can be found by noting that a uniform beam at $+\Delta/2$ minus one at $-\Delta/2$ leads to the surface current density (15) with b replaced by a. Although derived in the long wavelength limit, the above expressions remain valid up to frequencies well above the pipe cutoff[11]. The behaviour of $Z_T$ at low frequencies is discussed in the Appendix.

Measurements

The impedance of a loop of length $\ell$ = 30 cm and width $\Delta$ = 3.2 cm was measured in free space and inside a stainless-steel pipe of diameter $2b$ = 8.4 cm. At a frequency of 32 MHz, the inductive and resistive components were:

| L | R | |
|---|---|---|
| 0.2545 ± 0.0002 µH, | 0.0896 ± 0.002 Ω | inside pipe |
| 0.2843 ± 0.0002 µH, | 0.0742 ± 0.002 Ω | free space . |

From (2), the resistive component leads to a transverse impedance

$$\text{Re } Z_T = \frac{c}{\omega} \frac{R}{\Delta^2 \ell} = 75 \text{ }\Omega/\text{m}/\text{m} \pm 25\%$$

per metre of pipe, while a direct calculation using $\rho = 10^{-6}$ $\Omega \cdot$m gives

$$\text{Re } Z_T = 72 \text{ }\Omega/\text{m}/\text{m} .$$

The reduction in loop inductance leads to

$$\text{Im } Z_T = -29.1 \text{ k}\Omega/\text{m}/\text{m} \pm 2\% ,$$

while a direct calculation using (16) gives

$$\text{Im } Z_T = -34 \text{ k}\Omega/\text{m}/\text{m} .$$

The instrumental errors are indicated. The discrepancy between measurement and theory probably arises from the large value of $\Delta/2b$ = 0.38 used, the uncertainty in the loop dimensions, and possibly end effects.

In general, when measuring very small impedances, one should also subtract the radiation resistance from the loop measurements in free space. This is appreciable unless the loop is very short compared with a wavelength. Alternatively, one could place the loop in a circular copper pipe, for which the added impedance is easy to calculate. In addition, to some small extent, the current distribution over the cross-section of the loop conductor may change when the loop is inserted into a chamber, thus modifying its own impedance.

4. WINDOW-FRAME MAGNET

A window-frame magnet is sketched in Fig. 1 with a beam passing at a distance $x_0$ from the magnet centre line. Not shown are the return currents, which are assumed to flow along an external tank that encloses the magnet[*]. Several effects should be distinguished. First, there is a relatively large longitudinal impedance due to the induced flux that circulates within the core. It is mostly inductive,

---

[*] At high frequencies, the return currents may flow through the core, or along the conductors, etc., depending on the geometry of the magnet.

with a resistive component due to core losses. This flux does not link the magnet winding, and so is independent of the generator load $Z_g$. There is also a transverse impedance due to the differential flux induced in the core. Part of this arises from core losses[7,12,13], and part from coupling to the magnet winding. In the following, we compute only that part of $Z_L$ and $Z_T$ that arises from coupling with the magnet circuit.
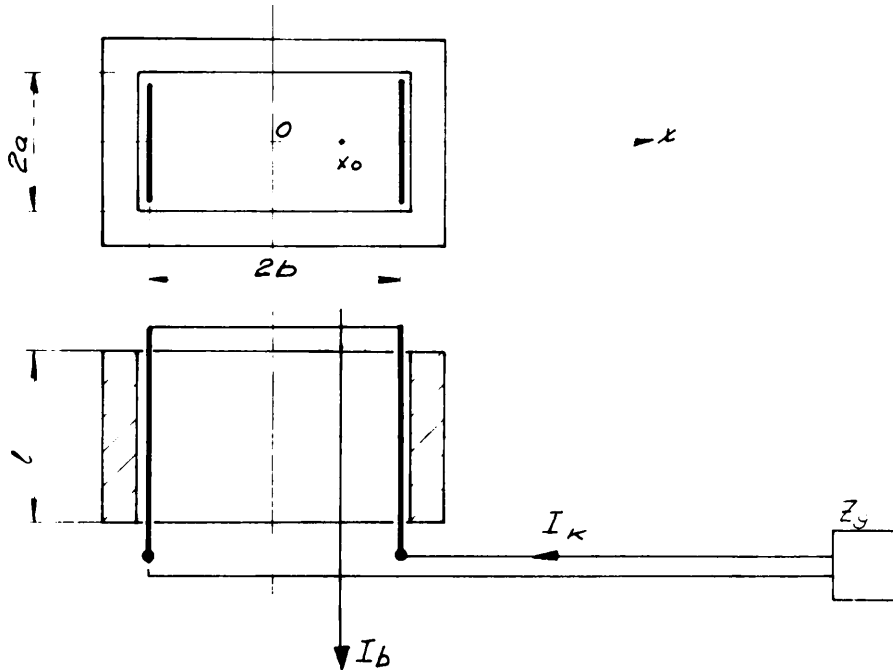


Fig. 1

The mutual inductance between magnet winding (index k) and beam circuit (index b) is easy to calculate. For a current $I_k$ in the magnet winding, the flux linking the beam circuit is

$$\phi_b = \frac{\mu_0 I_k}{2a} x_0 \ell \quad ,$$

regardless of how the return currents are distributed on the external tank. The mutual inductance between winding and beam is the same as that between beam and winding, with

$$M = \frac{\mu_0 \ell}{2a} x_0 \quad .$$

Therefore a beam of intensity I at $x_0$ induces the voltage

$$V_k = j\omega M(x_0) I$$

and current $I_k = V_k/Z_k$ in the winding. The impedance of the magnet circuit is

$$Z_k = j\omega L + Z_g \quad ,$$

where $L = \mu_0 b \ell / a$ and $Z_g$ is the generator impedance including cables. The current $I_k$ in turn induces the emf

$$V = -j\omega M(x) I_k = \frac{\omega^2 M(x) M(x_0) I}{Z_k}$$

at location x in the magnet, and therefore

$$Z_1(x, x_0) = \frac{\omega^2 M(x) M(x_0)}{Z_k} \quad . \tag{18}$$

The longitudinal and transverse impedances follow immediately from (4) and (5),

$$Z_L = \frac{\omega^2 \mu_0^2 x_0^2 \ell^2}{4a^2 Z_k} \qquad \Omega \quad , \tag{19}$$

$$Z_T = \frac{c\omega \mu_0^2 \ell^2}{4a^2 Z_k} \qquad \Omega/m \quad . \tag{20}$$

Note that $Z_L$ depends strongly on position, and is zero on the magnet centre line, so a relation such as (14) does not hold in this case.

We can check that measurements with a loop of width $\Delta$ also give (20). In this case, the mutual inductance between test loop and magnet winding is

$$M = \frac{\mu_0 \ell \Delta}{2a} \quad ,$$

so the additional impedance seen by the test loop is

$$Z = \frac{\omega^2 M^2}{Z_k} \quad ,$$

and (20) follows from the relation (2).

5. C-MAGNET

The results of the last section are easily extended to any C-core type magnet (Fig. 2). The magnetic field in the median plane is now a function of position,

$$B(x) = f(x) I_k$$

so

$$\phi_b = \ell \int_{-b}^{x} B(x') dx'$$

$$M = \ell \int_{-b}^{x} f(x') dx'$$

and

$$\frac{\partial M}{\partial x} = \ell f(x) \quad .$$

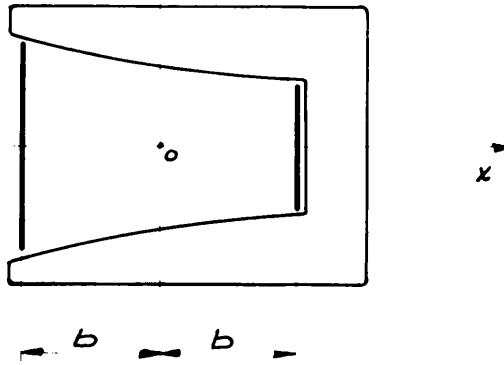The longitudinal and transverse impedances due to the magnet circuit are therefore

Fig. 2

$$Z_L = \frac{\omega^2 M^2 (x_0) \ell^2}{Z_k} \tag{21}$$

$$Z_T = \frac{c \omega f^2 (x_0) \ell^2}{Z_k} \tag{22}$$

For a constant gap height of 2a,

$$M = \frac{(x+b) \mu_0 \ell}{2a} \quad , \tag{23}$$

and

$$Z_L = \frac{\omega^2 (x_0+b)^2 \mu_0^2 \ell^2}{4a^2 Z_k} \tag{24}$$

$$Z_T = \frac{c \omega \mu_0^2 \ell^2}{4a^2 Z_k} \tag{25}$$

$$= \frac{c}{\omega b^2} Z_L \bigg|_{x_0=0}$$

The additional longitudinal impedance due to the flux that does not link the magnet circuit is very much reduced in this case by the air gap.

6. KICKER

A possible kicker is shown in schematic form in Fig. 3, with cables at either end and a beam passing at a distance $x_0$ from the axis. We assume that the beam return current flows either on the walls of the tank or on the surface of the "cold" conductor at -b. Not shown is the distributed capacitance that is usually added between "hot" and "cold" conductors to make the magnet circuit appear as a transmission line with the same characteristic impedance $Z_c$ as the cables. The loads $Z_1$ and $Z_2$ at the ends of the cable shown in Fig. 4 can be thyratrons, pulse-steepening lines, matched terminations, or other equipment.
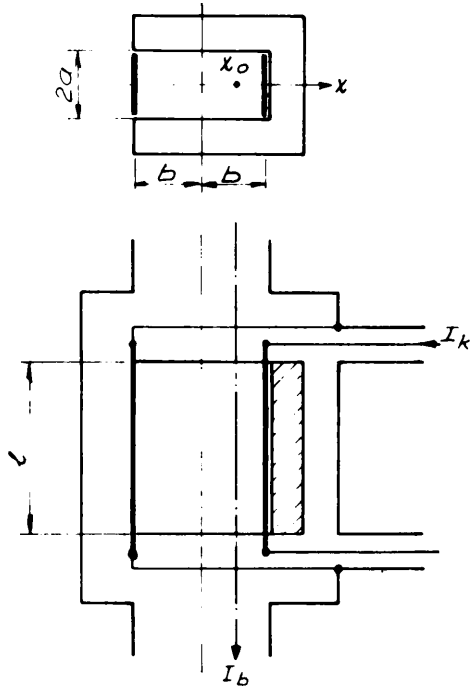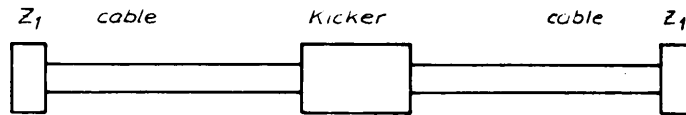
Fig. 3



Fig. 4

Steady excitation of the kicker with a wire at x produces sinusoïdal voltage and current wave forms along the line. If the kicker is short, we find as before

$$M = \frac{x + b}{2a} \mu_0 \ell \quad ,$$

while for a longer kicker, this must be multiplied by

$$G = \frac{\sin \theta/2}{\theta/2} \quad ,$$

where $\theta(\omega)$ is the electrical length of the kicker. In general, the finite propagation times of the beam or currents in the test conductor should also be included in G. Both can be neglected for the examples considered here and in the following section.

The current $I_k$ at the centre of the kicker induced by the beam current I is then

$$I_k = \frac{j\omega MGI}{Z_k} \quad ,$$

where

$$Z_k = Z_1' + Z_2' \, ,$$

and $Z_1'$ and $Z_2'$ are the load impedances transformed to the kicker centre, including dissipation in the cables and kicker. Finally, the impedances seen by the beam have the form (24) or (25) found before, but now multiplied by $G^2$.

## Measurements

The real parts of $Z_L$ and $Z_T$ were measured for a PS Booster ejection kicker module with equal lengths of cable on either side. Figure 5 shows the measured points and theoretical curve for the case of matched loads, $Z_1 = Z_2 = Z_c = 25 \, \Omega$. The agreement is reasonable considering the imperfect matching between kicker and cables, the poor RF qualities of the cables and terminations, and the fact that the kicker is not uniform along its length.

Figure 6 shows the measured results with one cable open-circuited and the other matched. In this case,

$$Z_k/Z_c = 1 + \left[\tanh \, (\alpha+j\beta)\ell\right]^{-1} \, ,$$

where the real part of $\tanh \, (\alpha+j\beta)\ell$ oscillates between $\tanh \alpha\ell$ and $(\tanh \alpha\ell)^{-1}$.

Figure 7 shows the measured results with both cables open-circuited. Now

$$Z_k/Z_c = 2\left[\tanh \, (\alpha+j\beta)\ell\right]^{-1} \, .$$

The peaks of $Z_L$ and $Z_T$ occur when there is a half an odd integer number of wavelength along the line.

## 7. APPLICATION TO THE PS BOOSTER

It has not yet been possible to measure *in situ* the fast injection kicker (IKF) or the ejection kicker (EK), so the following estimates are based on the measurements discussed in the last section.

IKF is a single module, matched at one end, and about twice as long but otherwise similar to an EK module. The impedances should therefore be about four times those shown in Fig. 6, but falling to zero around 12 MHz, with a maximum value of $Z_T$ around 40 k$\Omega$/m. The longitudinal impedance $Z_L$ varies quadratically across the aperture from zero on the side closest to the machine centre, and with peak values on the axis of around 20 $\Omega$.

EK consists of four modules connected to a common steepening line and a common spark gap as shown in Fig. 8. In the ring, the four modules are reversed in pairs. For symmetric modes, with all modules driven in phase, $Z_T$ is about four times the values shown in Fig. 7b, but somewhat reduced by damping in the steepening line, and with different resonant frequencies that depend on the pulse steepening line and installed cable lengths.
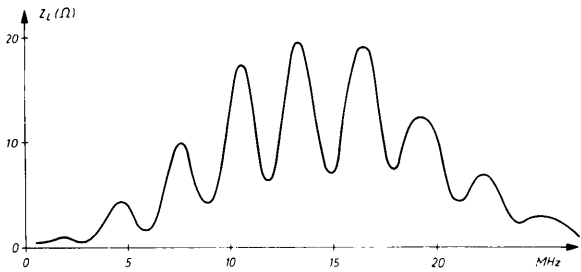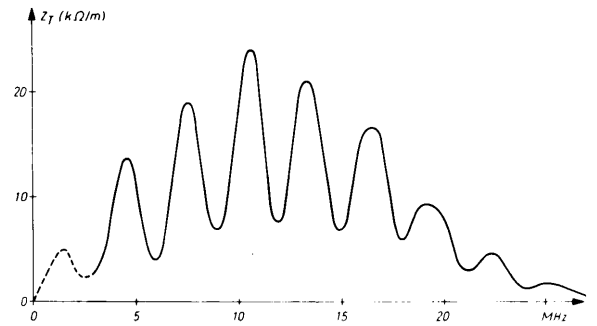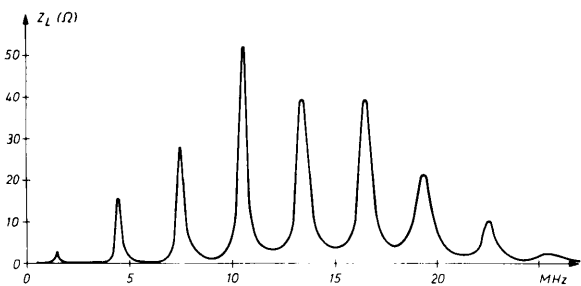
a)                    Fig. 5                    b)



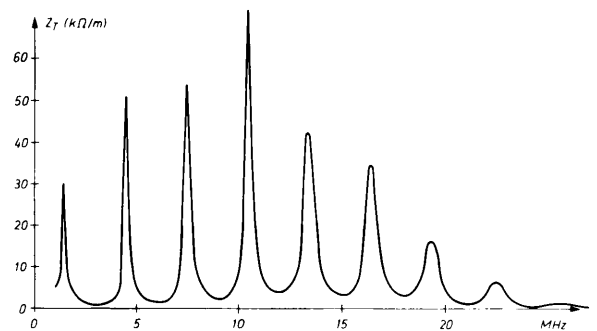a)                    Fig. 6                    b)



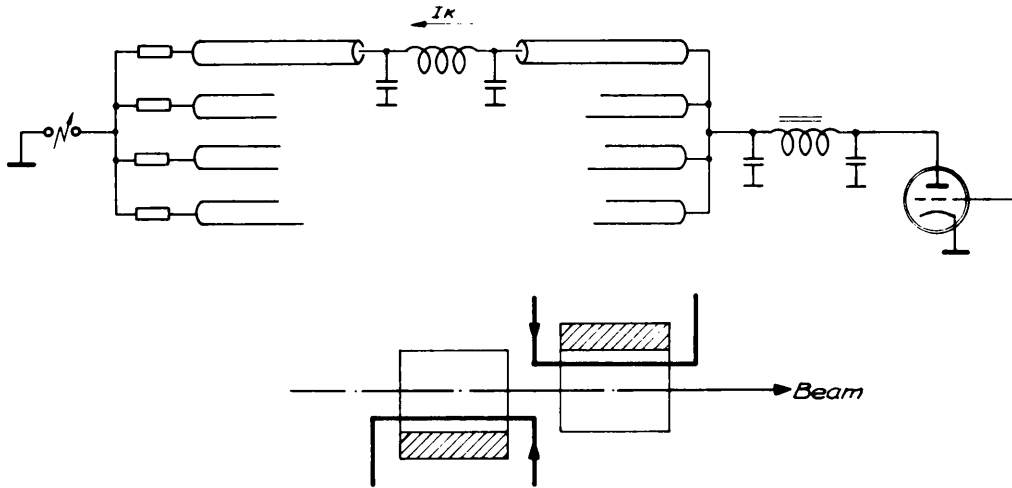a)                    Fig. 7                    b)
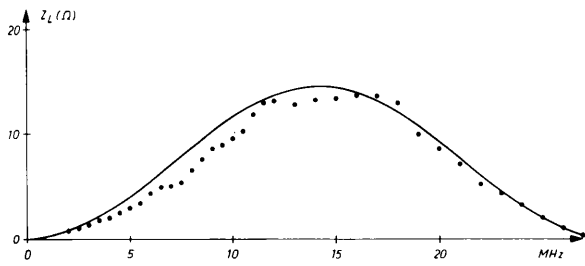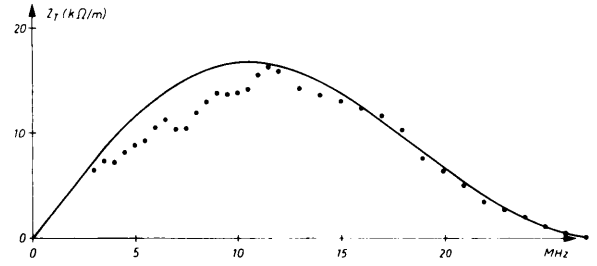
Fig. 8

The envelope of the expected peak impedances of the kickers are shown in
Fig. 9, together with the resistive-wall impedance for the 52 m of thin wall cor-
rugated vacuum chamber in the PSB bending magnets. As can be seen, the ejection
kicker impedance is considerably larger than the resistive-wall impedance for
frequencies above 1 MHz. This could explain the horizontal instabilities observed
in the PS Booster[14]. A similar instability has been observed in the KEK
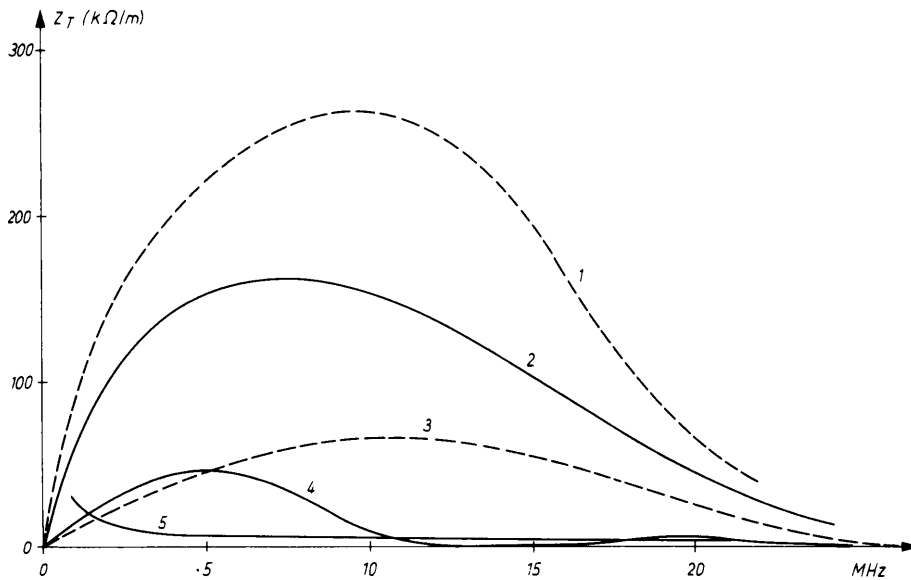Booster[15].



Fig. 9

1. Envelope of impedance peaks for four EK modules with cables
   open-circuited.
2. Estimated envelope of EK impedance peaks with pulse steepening
   line and spark gap connected.
3. EK impedance with all cables matched.
4. Estimated envelope for IKF.
5. Resistive wall impedance.

Because the modules are reversed in pairs, the longitudinal impedance is zero on axis for the symmetric mode, and rises quadratically as the beam is displaced to either side. In the limiting position, the beam couples to only two of the four modules. The undriven modules act as loads in this case, so the resulting total impedance is similar to that of a single module, with an expected peak value of around 200 $\Omega$.

There are also antisymmetric modes, with two modules driven in opposite phase. In this case $Z_T$ is zero and $Z_L$ is independent of position and about four times the values shown in Fig. 6a, with an expected peak value of around 80 $\Omega$.

## Acknowledgements

## REFERENCES

1) F.J. Sacherer, Transverse bunched beam instabilities - theory, 9th Internat. Conf. on High-Energy Accelerators, Stanford, 1974 (U.S. Atomic Energy Commission, Washington, 1974), p. 347.

2) A. Faltens et al., An analogue method for measuring the longitudinal coupling impedance of a relativistic particle beam with its environment, 8th Internat. Conf. on High-Energy Accelerators, CERN, 1971 (CERN, Geneva, 1971), p. 338.

3) H.H. Umstätter, On the measurement and interpretation of coupling impedance data in the frequency and time domain, 6th National Particle Accelerator Conf., Washington, 1975 (IEEE, New York, 1975), p. 1875.

4) P. Bramham, Laboratory measurement of RF resonances and impedances in the ISR vacuum chamber components, CERN-ISR-RF/76-49 (1976).

5) P.B. Wilson et al., Comparison of measured and computed loss to parasitic modes in cylindrical cavities with beam ports, 7th National Particle Accelerator Conf., Chicago, 1977 (IEEE, New York, 1977), p. 1496.

6) W. Schnell, A relation between longitudinal and transverse instability thresholds for a beam traversing a resonant cavity, CERN-ISR-RF/70-7 (1970).

7) D. Möhl, Equipment responsible for transverse beam instability in the PS, CERN internal note MPS/DL/Note 74-6 (1974).

8) W. Schnell and B. Zotter, A simplified criterion for transverse stability of a coasting beam, and its application to the ISR, CERN-ISR-GS-RF/76-26 (1976).

9) L.J. Laslett, V.K. Neil and A.M. Sessler, Transverse resistive instabilities of intense coasting beams in particle accelerators, Rev. Sci. Instrum. 36, 436 (1965).

10) E. Keil, Intersecting storage rings, CERN 72-14 (1972).

11) B. Zotter, High-frequency effects on the transverse resistive wall instability in particle storage rings, CERN 69-16 (1969).

12) B. Zotter, Transverse oscillations of a relativistic particle beam in a laminated vacuum chamber, CERN 69-15 (1969).

13) A.G. Ruggiero, The head-tail effect in the NAL booster, FNAL report FN-248 (1972).

14) H. Schönauer, private communication.

15) Y. Kimura et al., Transverse coherent instability in the KEK booster, 10th Internat. Conf. on High-Energy Accelerators, Serpukhov, 1977; see KEK Preprint 77-8 (1977).

$Z_T$ IN THE LIMIT OF LOW FREQUENCIES

For frequencies such that the skin depth is greater than the wall thickness d, $\Re \to \rho/d$. For even lower frequencies, the wall currents induced by the beam or test loop approach zero. This can be seen from the equivalent circuit diagram shown below, where the subscript L refers to the loop and W to the wall[*].
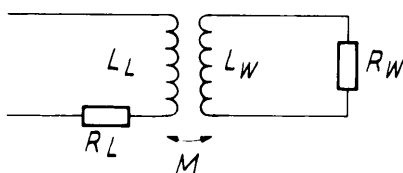


$$M = \frac{2\mu_0}{\pi} \frac{\Delta}{2b} \ell$$

$$L_W = \frac{2\mu_0}{\pi} \ell$$

$$R_W = 8 \frac{\rho}{d} \frac{\ell}{2\pi b}$$

The current induced in the wall is given by

$$j\omega M I_L = (R_W + j\omega L_W) I_W ,$$

so

$$I_W = \frac{j\omega M I_L}{R_W + j\omega L_W} ,$$

which approaches zero for frequencies below

$$\omega_c = \frac{R_W}{L_W} = \frac{2}{\mu_0} \frac{\rho}{bd} .$$

The voltage induced in the loop by the wall current is

$$Z I_L = -j\omega M I_W ,$$

so the added loop impedance is

$$Z = \frac{\omega^2 M^2}{R_W + j\omega L_W}$$

$$= \frac{-j\omega L_W + R_W}{1 + (\omega_c/\omega)^2} \frac{\Delta^2}{4b^2} .$$

The transverse impedance obtained from (2) is the same as that found before [Eqs. (13) and (17)], except that the component due to the wall current is multiplied by $\omega^2/(\omega^2 + \omega_c^2)$. For a stainless-steel vacuum chamber of 5 cm radius, 1 mm thickness, and $\rho = 10^{-6}$ $\Omega \cdot$m, the critical frequency $f_c$ is 5 kHz.

---

[*] We assume a circular pipe of radius b. The effective wall resistance $R_W$ is a factor of 8 larger than the d.c. resistance of a pipe of length $\ell$, radius b, and thickness d: a factor of 2 arises because the current flows down one side of the pipe and returns on the other side, and a factor of 4 because the cos $\theta$ distribution restricts the current in one direction to effectively $\frac{1}{4}$ of the pipe circumference.